ChemComm

A self-calibrating dual responsive platform for sensitive detection of sulfite and sulfonic derivatives based on a robust Hf(IV) metal−organic framework

Journal:	*ChemComm*
Manuscript ID	CC-COM-10-2019-007869.R1
Article Type:	Communication

Journal Name

COMMUNICATION

A self-calibrating dual responsive platform for sensitive detection of sulfite and sulfonic derivatives based on a robust Hf(IV) metal–organic framework

Received 00th January 20xx,
Accepted 00th January 20xx

DOI: 10.1039/x0xx00000x

www.rsc.org/

Kai Xing,[ab] Rui-Qing Fan,*[a] Xiao-Yuan Liu,[bc] Shuang Gai,[a] Wei Chen,[a] Yu-Lin Yang*[a] and Jing Li*[bc]

A robust hafnium-based metal organic framework Hf-PBTA with sensitive and self-calibrating dual-emissive fluorescence response toward sulfite and sulfonic derivatives, including antibiotic sulfamethazine, has been developed, which shows a fast detection of sulfite ions at a concentration as low as 76 ppb. The opposite response tendency from two radiative pathways towards aromatic sulfonic molecules and sulfite anion stems from the synergistic effect of pyridine protonation effect, π-π stacking interaction and intramolecular twist motion.

The drinking water has a direct and intimate impact to human life. The contaminants in drinking water have become a serious risk to health of living beings and ecosystem.[1, 2] Among them, hazardous pollutants such as sulfonic derivatives, widely utilized in feed additives,[3] pharmaceutical and personal care products[4] are usually generated from the excessive use and inefficient disposal, and this scenario is getting worse because of the incremental population and global industrialization.[5, 6] Thus, it is imperative to develop efficient methods to monitor and remove such pollutants from drinking water systems. Various analytical techniques have been used to detect sulfonic derivatives over the past decades.[7] Besides the direct instrument analysis, chemical sensor based methods have also been developed.[8] Notably, the fluorescence based methods are particularly attractive due to several unique merits, including simplicity, high sensitivity and fast response.[9]

Most of the reported fluorescent sensors rely on the changes of single fluorescence signal (e.g. intensity enhancement or quenching),[10-12] which suffers from low selectivity.[13] In contrast, self-calibrating sensors have high signal-to-background and low sensitivity to external factors, which not only can monitor host-guest interactions through variation of fluorescence intensity ratio of different emission centers,[14] but also can improve selectivity and sensitivity for more accurate and reliable quantification of specific targets,[15] However, ratiometric fluorescent sensors with self-calibrating character for sulfonic derivatives are rare, because it remains a significant challenge to design two emissive centers with optimal performance and to control other factors, especially in complex realistic detection systems.

As a group of promising sensor candidates, fluorescent hafnium metal-organic frameworks (Hf-MOFs) made of highly connected metal oxygen clusters and diverse organic ligands are well known for their stability and durability owing to the high dissociation enthalpies of a typical Hf–O bond (802 kJ mol^{-1}),[16] which is desirable for real-world applications. In addition, the tunable pore shape and decorated active sites also increase the modularity to control the interactions between the target analytes and the framework.[17] Therefore, the strategy that fully utilizes the conjugated system of π electron, the hydrogen binding sites of functional groups and the twisting motions within the ligand is feasible to design and construct Hf-MOF based sensors with self-calibrating dual-emissive ratiometric sensing behavior.

Herein, we report the solvothermal synthesis of a Hf-MOF (**Hf-PBTA**) (H_4PBTA = 4,4′,4″,4‴-(4,4′-(1,4-phenylene)bis(pyridine-6,4,2-triyl))-tetrabenzoic acid) and its ratiometric and self-calibrating fluorescence based sensing of sulfonic derivatives. The overall crystal structure of **Hf-PBTA** is isoreticular to that of BUT-15.[18] To confirm this, the optimization of **Hf-PBTA** was conducted based on the reported BUT-15 structure replacing Zr^{4+} by Hf^{4+}. The result from Rietveld refinement shows an excellent agreement between the simulated and experimental PXRD patterns (Fig. S1). Hafnium forma a typical Hf_6 oxide cluster node which is connected by tetratopic ligand to form a 3D framework with a quadrangular shape (I: 9 × 16) and a waterdrop shaped (II: 17 ×

[a] MIIT Key Laboratory of Critical Materials Technology for New Energy Conversion and Storage, School of Chemistry and Chemical Engineering, Harbin Institute of Technology, Harbin, 150001, P. R. China.
[b] Department of Chemistry and Chemical Biology, Rutgers University, 123 Bevier Road, Piscataway, New Jersey, 08854, United States.
[c] Hoffmann Institute of Advanced Materials, Shenzhen Polytechnic, 7098 Liuxian Blvd, Nanshan District, Shenzhen, 518055, P.R. China

† Electronic Supplementary Information (ESI) available: Experimental details, PXRD patterns, TGA, emission spectra and supplementary figures. See DOI: 10.1039/x0xx00000x

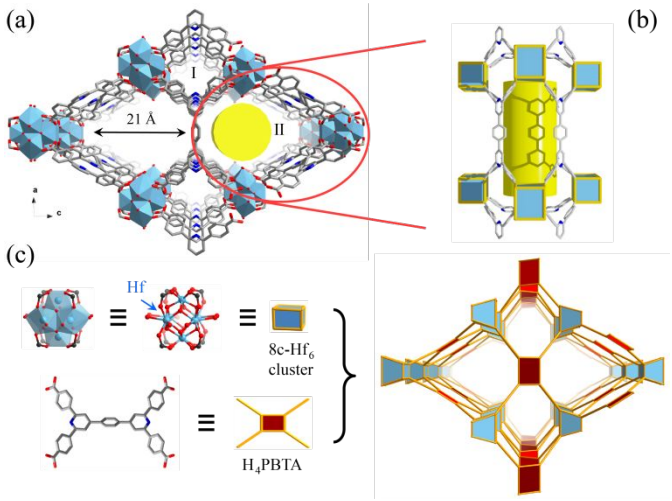

Fig. 1 (a) The 3D structure of **Hf-PBTA**; (b) The water-drop shaped 1D channel along the *b* axis; (c) The eight connected inorganic hafnium oxygen cluster, four connected organic H_4PBTA ligand and the simplified topological ***sqc-a*** network.

21 Å^2) channels (Fig. 1a and 1b), which can be simplified as a 4,8-c binodal ***sqc-a*** topological network (Fig. 1c). The phase purity of **Hf-PBTA** and its chemical stability in water and in acid/alkaline aqueous solutions were confirmed by PXRD analysis (Fig. S2 and S3) at room temperature. The crystallinity of the framework was retained for the pH range of 1-10 after being soaked in the solution for 48 h. The structure was stable up to 507 °C in nitrogen atmosphere (Fig. S5), which is ~50 °C higher than that of the Zr isostructural MOF because of the higher Hf-O dissociation enthalpy.

The optical properties were investigated by UV-Vis and photoluminescence spectroscopic analysis. As shown in Fig. S7, the UV-Vis absorption band of **Hf-PBTA** is centered at 330 nm which is narrowed as a result of coordination with metal ion to forming framework (Δ_{FWHM} = 84 nm). Solid state photoluminescence spectra show that both **Hf-PBTA** and the ligand display two emission bands (450 nm and 544 nm for ligand; 426 nm and 560 nm for **Hf-PBTA**) under excitation of 320 nm at room temperature. The lifetime of **Hf-PBTA** in solid state was estimated to be 10.65 ns. According to the reported studies (Table S1), the high energy (HE) band and low energy (LE) emission band could be assigned to organic ligand based the π → π* and n → π* electron transition, respectively, which is also supported by the calculated electron density distribution of ligand (Fig. S9). Additionally, the emission intensity of **Hf-PBTA** was found to be steady in aqueous solution (Fig. S10) for one week, implying a good photo-stability. Notably, the blue shift of emission band in aqueous solution compared to its solid-state can be attributed to weaker hydrogen bonding interactions and decrease of the interchromophore coupling.[19] Combining its unique fluorescence behavior with high water stability and permanent porosity, we considered **Hf-PBTA** a suitable candidate and explored its self-calibrating ratiometric sensing behavior toward sulfonic derivatives in aqueous medium.

The fluorescent sensing performance was evaluated on two typical categories containing sulfonic group substituted derivatives: (1) the aliphatic sulfonic molecules, such as aminomethanesulfonic acid (AMSA) and 1-heptanesulfonic acid sodium salt (HSA); (2) the aromatic sulfonic derivative, such as benzenesulfonic acid (BSA) and *p*-toluenesulfonic acid (TSA) (Scheme S2). For each analyte, fluorescence intensity was recorded after adding 1 mM selected analyte aqueous solution to sensing suspension in an incremental manner. The Hf-PBTA crystals were uniformly dispersed with a morphology of octahedral shape and an average size of ~500 nm (Fig. S11).

As shown in Figs. S12 and S13, the addition of aliphatic sulfonic molecules had no influence on the fluorescence intensity even with high concentrations. Nevertheless, continuous addition of aromatic sulfonic molecules led to gradual decrease in the intensity of the high energy band and increase in the intensity of the low energy band (Figs. S14 and S15). Setting the BSA as an example (Fig. 2a), the intensity ratio of I_{480}/I_{388} displays a linear relationship with the BSA concentrations in the range of 0-50 μM. The limit of detection (LOD) was calculated to be 0.192 ppm on the basis of 3σ/m (Fig. S14). Furthermore, about 90% of the equilibrium intensity ratio was reached in 40 seconds (Fig. S17) without stirring, indicating a relatively fast response.[20] The observed phenomenon may be attributed to the energy transfer because of the strong overlap between the absorption spectrum of **Hf-PBTA** and emission spectra of aromatic sulfonic molecules (Figs. S18-S20), while none of the aliphatic molecules exhibit such overlaps.[21] In addition to the long-range order energy transfer, the intimate gust-host interactions should be taken into consideration as well. From the structure of aromatic sulfonic molecules, the possible interacting moiety or influential factors may come from the following three aspects: (1) the aromatic conjugation system with rich π electricity; (2) the protonation effect caused by acid environment; (3) the potential hydrogen binding interaction with substituted sulfonic anion group.

Starting from the delocalization of conjugation system of **Hf-PBTA**, the large size and aromatic ring of the aromatic sulfonic derivatives might induce the π-π stacking interaction with the wall of the waterdrop-shaped channels within the framework, resulting in the quenching effect on π* → π decay transition and the enhancement on the radiative pathway of 480 nm emission band, which could be supported by the similar response behavior towards Pyridine-3-sulfonic acid (PSA) (Fig. S16) in 0-20 μM. Additionally, this effect is synergistic with the influence from sulfonic group, which can be proven by selective fluorescent response to aromatic molecules without sulfonic group and its deprotonated species (Figs. S21-S23). Here, the different linear sensing range stems from various electron densities of conjugated systems in analytes. Secondly, on account of the easy protonation of the nitrogen atoms of the pyridine part within the ligand in acidic environment,[22] the contrast experiment was carried out and the fluorescence was recorded in aqueous solution with pH variation to figure out the impact on the sensitivity towards proton. As shown in Fig. S24, the peak at HE band decreases, while the intensity of LE band increases. The trend of these two emissions is similar to that of aromatic sulfonic molecules but acid environment has more influence on the intensity ratio of I_{480}/I_{388} under same

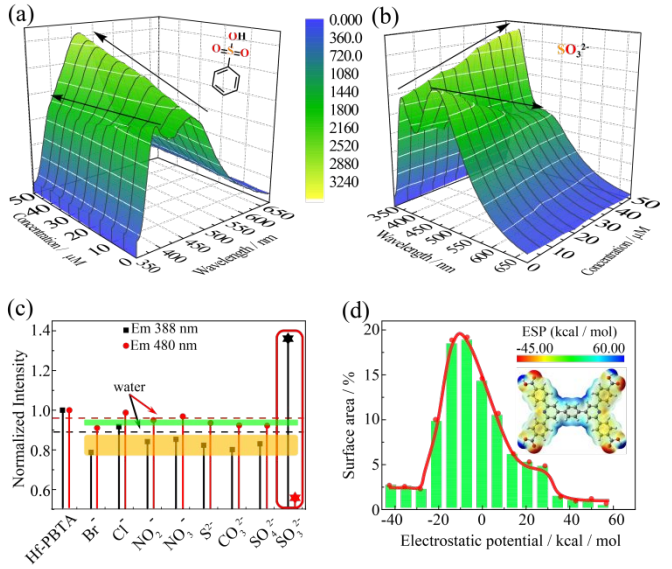

Fig. 2 (a) 3D fluorescent emission of **Hf-PBTA** with incremental addition of benzenesulfonic acid (BSA) (Ex = 330 nm); (b) 3D fluorescent emission of **Hf-PBTA** with incremental addition of sulfite anion (SO_3^{2-}) (Ex = 330 nm); (c) The influence of other anions and water to the two emission bands of **Hf-PBTA** (black square and star: normalized intensity of Em_{388}; red circle and star: normalized intensity of Em_{480}); (d) The surface area percent in each electrostatic potential surface range on the *vdW* surface of H_4PBTA ligand (Inset: ESP mapped molecular *vdW* surface of H_4PBTA ligand).

concentration with aromatic sulfonic analytes, indicating that the protonation of H_4PBTA ligand has a certain influence on the dual-emission of MOF but other aspect may contribute to the emission in a more dominant way.

In order to demonstrate the influence of sulfonic anion group, the fluorescence response of **Hf-PBTA** towards inorganic sulfite anion was measured. It was noted that the emission band centered at 388 nm rose and that at 480 nm fell (Fig. 2b), which is an exactly opposite tendency comparing with the response behavior towards aromatic sulfonic species. Simultaneously, the significant increase in the relative proportion of π → π* transition in the emission spectrum is also in support of the crucial influence of sulfite anion. Comparing with other selected anion analytes, the **Hf-PBTA** displays the most efficient response behavior and sensitivity towards sulfite anions based on a quantitative analysis via fluorescent titration (Fig. S25). The intensity ratio (I_{388}/I_{480}) also linearly correlates with the low concentration range, and deviates to the exponential relationship at higher concentrations. The LOD was calculated to be 76 ppb. Accordingly, the solution color shifts from cyan to light-blue with Commission Internationale d'Eclairage (CIE) coordinates varying from (0.21, 0.28) to (0.21, 0.23), where the green (G)/blue (B) intensity ratios of the image (taken by smartphone) changed from 1.06 to 0.76 visually by the aid of a color-scanning evaluation application (Fig. S26). In addition, **Hf-PBTA** displays a good selectivity and anti-interference ability towards other anions. As shown in Fig. S28, other anions gave negligible effect on the fluorescence of **Hf-PBTA** and only very small influence was observed with water (Fig. 2c). Even when other anions with equal concentration were present in the solution, the intensity ratio of I_{388}/I_{480} remained to increase after addition of SO_3^{2-} anion, which confirmed that sulfite anion generates stronger interaction with the framework (Figs. S28 and 29). The above results also suggest that the two decay pathways of the **Hf-PBTA** may be influenced differently upon the addition of different sulfonic derivatives.

Notably, the size of sulfite anion is smaller than sulfonic derivatives, so the type II channel might be more preferential to interact with. To confirm this, we calculated the electrostatic potential (ESP) on molecular surface which is critical for understanding and predicting gust-host intermolecular interaction site.[23] Accordingly, the maxima and minima points were conducted by Multiwfn software.[24] From the ESP mapped van der Waals (*vdW*) surface of H_4PBTA ligand (Fig. 2d), the pyridine ring with more negative electrostatic values was most active moiety to interact with the gust anions upon the carboxyl group occupied by Hf-oxygen cluster. To gain better insight to the interaction and the sensing behavior, the density functional theory (DFT) calculation was applied here. As shown in Fig. 3, the introduction of the sulfite anion plays a key role in configuration of H_4PBTA in ground and excited state, leading the dihedral angles between the phenyl rings and pyridine ring (defined as ∠ A-Py, B-Py, C-Py, D-Py and E-Py) changed significantly. For H_4PBTA with two sulfite anions system, the ∠ outer benzene-Py exhibited an obvious decrease upon excitation. For excited H_4PBTA with four sulfite anions system, the dihedral angles of ∠A-Py, D-Py and E-Py showed a certain increase to some extent, however, the whole co-planarity was still improved comparing with the ground state. Moreover, the significant decrease of ∠C-Py (Δ = 31°) in excited state with the concentration increase, which was also beneficial to the decay channel of π* → π transition. The twist motion could be attributed to the restriction caused by hydrogen binding interaction between the protonated sulfite anion and pyridine moiety[25, 26] and dipole−dipole intermolecular interactions between analytes.[27] These interactions would also reduce the transition of n electron and hinder the n-π* electronic transitions.[28] Therefore, the ligand might adjust the configuration itself and further change de-excitation channels of excitation state, resulting in increased

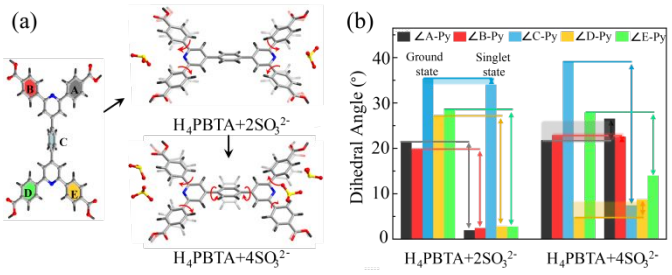

Fig. 3 (a) The molecular configuration variation of H_4PBTA ligand after interacting with two and four sulfite anions in ground state and singlet state respectively; (b) The dihedral between the benzene ring (A-E)and pyridine ring (Py) with two and four sulfite anions.

intensity of HE band and decreased intensity of LE band.

The excellent stability, sensitivity and selectivity prompted us to evaluate the use of **Hf-PBTA** to quantitatively determine the trace amount of aromatic sulfonic compounds, such as the sulfamethazine (SMA), in a water system. This antibiotic is widely used in treatment of bacterial infection for creatures, however, the contamination from antibiotic residues in drinking water or even animals would lead to severe diseases,[29, 30] which is consequently to be desired to detect in a sensitive way. Therefore, the emissive intensity ratio (I_{480}/I_{388}) of **Hf-PBTA** was significantly enhanced upon exposure to the SMA containing water (Fig. S30). The LOD of **Hf-PBTA** was calculated to be 0.668 ppm (Table S2) based on the linear relationship between the response signal and concentration, where the π-π aromatic conjugation effect was mainly responsible among the three synergistic aspects due to the nearly neutral pH and another substituted aromatic part of SMA.

In summary, the highly sensitive and ratiometric sensing platform towards sulfite and sulfonic derivatives has been constructed based on a robust **Hf-PBTA**. Notably, the Hf-MOF-based sensor material displays opposite response towards aromatic sulfonic derivative and sulfite anion. By combining the pyridine protonation effect, π-π stacking interaction and twist motion induced by hydrogen binding interaction, helpful insight on the observed fluorescence changes has been obtained. The robust **Hf-PBTA** also exhibits sensitive detection to the antibiotic in aqueous solution. This work serves a good example of self-calibrating fluorescent ratiometric sensor for possible applications in monitoring hazardous chemical species in aqueous solutions.

Kai Xing, Ruiqing Fan, Wei Chen, Shuang Gai and Yulin Yang thank the National Natural Science Foundation of China (Grant No. 21873025 and 21571042) for their support. Kai Xing gratefully acknowledges the financial support of the China Scholarship Council (CSC, 201806120319) to support his study at Rutgers University. The RU team acknowledge the partial support the National Science Foundation (Grant No. DMR-1507210).

Conflicts of interest

The authors declare no competing financial interests.

Notes and references

1 P. M. Chapman, *Environ. Int.*, 2007, **33**, 492-501.
2 P. L. Wang, L. H. Xie, E. A. Joseph, J. R. Li, X. O. Su and H. C. Zhou, *Chem. Rev.*, 2019, **119**, 10638-10690.
3 P. W. Seo, N. A. Khan, Z. Hasan and S. H. Jhung, *ACS Appl. Mater. Interfaces*, 2016, **8**, 29799-29807.
4 S. Castiglioni, R. Bagnati, R. Fanelli, F. Pomati, D. Calamari and E. Zuccato, *Environ. Sci. Technol.*, 2006, **40**, 357-363.
5 Q. Q. Zhang, G. G. Ying, C. G. Pan, Y. S. Liu and J. L. Zhao, *Environ. Sci. Technol.*, 2015, **49**, 6772-6782.
6 P. Samanta, A. V. Desai, S. Let and S. K. Ghosh, *ACS Sustainable Chem. Eng.*, 2019, **7**, 7456-7478.
7 K. Wu, J. Guo and C. Wang, *Chem. Commun.*, 2014, **50**, 695-697.
8 Y. Takashima, V. M. Martinez, S. Furukawa, M. Kondo, S. Shimomura, H. Uehara, M. Nakahama, K. Sugimoto and S. Kitagawa, *Nat. Commun.*, 2011, **2**, 168.
9 L. E. Kreno, K. Leong, O. K. Farha, M. Allendorf, R. P. Van Duyne and J. T. Hupp, *Chem. Rev.*, 2012, **112**, 1105-1125.
10 J. Zhang, S. B. Peh, J. Wang, Y. Du, S. Xi, J. Dong, A. Karmakar, Y. Ying, Y. Wanga and D. Zhao, *Chem. Commun.*, 2019, **55**, 4727-4730.
11 Z. Hu, B. J. Deibert and J. Li, *Chem. Soc. Rev.*, 2014, **43**, 5815-5840.
12 W. P. Lustig, S. Mukherjee, N. D. Rudd, A. V. Desai, J. Li and S. K. Ghosh, *Chem. Soc. Rev.*, 2017, **46**, 3242-3285.
13 Y. Q. Wang, T. Zhao, X. W. He, W. Y. Li and Y. K. Zhang, *Biosens. Bioelectron.*, 2014, **51**, 40-46.
14 R. Gui, H. Jin, X. Bu, Y. Fu, Z. Wang and Q. Liu, *Coord. Chem. Rev.*, 2019, **383**, 82-103.
15 S. Krause, V. Bon, U. Stoeck, I. Senkovska, D. M. Tobbens, D. Wallacher and S. Kaskel, *Angew. Chem., Int. Ed.*, 2017, **56**, 10676-10680.
16 J. A. Kerr, *In CRC Handbook of Chemistry and Physics, 81st ed.; Lide, D. R., Ed.; CRC Press: Boca Raton, , FL, 2000.*, Lide, D. R., Ed.; CRC Press: Boca Raton, FL, 2000.
17 R. W. Huang, Y. S. Wei, X. Y. Dong, X. H. Wu, C. X. Du, S. Q. Zang and T. C. W. Mak, *Nat. Chem.*, 2017, **9**, 689-697.
18 B. Wang, Q. Yang, C. Guo, Y. Sun, L. H. Xie and J. R. Li, *ACS Appl. Mater. Interfaces*, 2017, **9**, 10286-10295.
19 K. C. Stylianou, R. Heck, S. Y. Chong, J. Bacsa, J. T. A. Jones, Y. Z. Khimyak, D. Bradshaw and M. J. Rosseinsky, *J. Am. Chem. Soc.*, 2010, **132**, 4119-4130.
20 X. Zhou, J. Liu, C. Wang, P. Sun, X. Hu, X. Li, K. Shimanoe, N. Yamazoe and G. Lu, *Sens. Actuators, B*, 2015, **206**, 577-583.
21 S. Pramanik, C. Zheng, X. Zhang, T. J. Emge and J. Li, *J. Am. Chem. Soc.*, 2011, **133**, 4153-4155.
22 S. L. Hou, J. Dong, M. H. Tang, X. L. Jiang, Z. H. Jiao and B. Zhao, *Anal. Chem.*, 2019, **91**, 5455-5460.
23 J. S. Murray and P. Politzer, *Wiley Interdisciplinary Reviews: Computational Molecular Science*, 2011, **1**, 153-163.
24 T. Lu and F. Chen, *J. Comput. Chem.*, 2012, **33**, 580-592.
25 A. Mallick, A. M. El-Zohry, O. Shekhah, J. Yin, J. Jia, H. Aggarwal, A. H. Emwas, O. F. Mohammed and M. Eddaoudi, *J. Am. Chem. Soc.*, 2019, **141**, 7245-7249.
26 A. M. El-Zohry, A. Alturki, J. Yin, A. Mallick, O. Shekhah, M. Eddaoudi, B. S. Ooi and O. F. Mohammed, *J. Phys. Chem. C*, 2019, **123**, 5900-5906.
27 J. H. Carter, X. Han, F. Y. Moreau, I. da Silva, A. Nevin, H. G. W. Godfrey, C. C. Tang, S. Yang and M. Schroder, *J. Am. Chem. Soc.*, 2018, **140**, 15564-15567.
28 Y. Sun, C. Zhong, R. Gong, H. Mu and E. Fu, *J. Org. Chem.*, 2009, **74**, 7943-7946.
29 A. U. Rajapaksha, M. Vithanage, M. Ahmad, D. C. Seo, J. S. Cho, S. E. Lee, S. S. Lee and Y. S. Ok, *J. Hazard. Mater.*, 2015, **290**, 43-50.
30 B. Wang, X. L. Lv, D. Feng, L. H. Xie, J. Zhang, M. Li, Y. Xie, J. R. Li and H. C. Zhou, *J. Am. Chem. Soc.*, 2016, **138**, 6204-6216.

TOC Entry

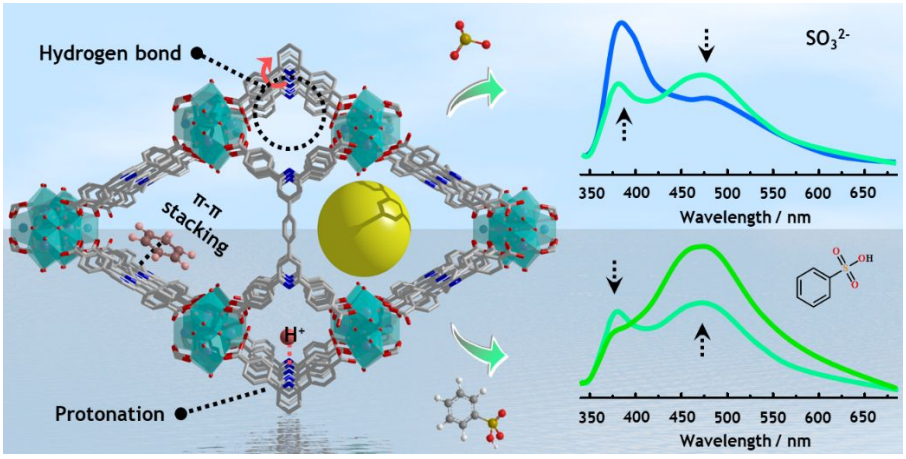

A robust Hf-MOF exhibits highly-sensitive and opposite ratiometric fluorescence response towards sulfite and sulfonic derivatives.